

# Numerical Analysis on The Effect of Barge Motion to Jacket Lifting Process During Decommissioning

Murdjito<sup>1</sup>, Vebby A. Kurniawan<sup>2</sup>, Raditya D. Riyanto<sup>3</sup>, Rudi W. Prastianto<sup>4</sup>

(Received: 08 February 2023 / Revised: 09 February 2023 / Accepted: 02 March 2023)

**Abstract**— Offshore structure decommissioning is mandatory when an offshore oil and gas platform reaches the end of its service life. There are no less than 450 fixed offshore steel structures in Southeast Asia, and by 2030, more than 200 offshore fields will be terminated and need to be decommissioned. From an operational aspect, the decommissioning process is simply an inverse of installation. However, due to the structures' age and the uncertainties of the structural performance, the simple operation can be an obfuscating process. This paper discusses one of the most crucial processes during decommissioning: lifting. The dynamic performance of a lifted jacket in several rigging variations is investigated. We use a standard stern crane HLV (Heavy Lift Vessel) to simulate the process, with several wave attack angles. Sea condition is according to DNVGL benign wave during marine operation, with random waves generated using the JONSWAP spectrum. Coupled dynamics of HLV and jacket motion are analyzed.

**Keywords**— Decommissioning, Heavy lift vessel, Numerical analysis, Offshore jacket lifting.

## I. INTRODUCTION

Southeast Asia's oil and gas supply comes 60% from offshore fields located in shallow water, less than 450 m meters in depth. There are no less than 450 fixed steel offshore oil and gas facilities operating in Southeast Asia Region, and most of them are aged platforms with more than 30 years of operation. (International Energy Agency, 2019). Almost 40% of all offshore oil and gas fields have been operating for more than 20 years. In Indonesia specifically, the number will be higher than Southeast Asia's average, at 55%. By 2030, more than 200 offshore fields will have terminated their production and need to be decommissioned. Learning from past events, the challenges for decommissioning came from many aspects, including financial, environmental, and operational aspects [1].

The financial aspect was discussed thoroughly, including cost estimation of fixed platforms removal in the U.S. Gulf of Mexico. Circa January 2013, the cost to remove a single fixed deepwater structure is estimated to be worth \$2.4 billion [2]. The estimation was corrected due to the lack of transparency on decommissioning cost data. However, the decommissioning process is an obligation to the operator due to the state regulation to

safely abandon and remove all the oil and gas operation apparatus, including the environmental recovery after the exploration and exploitation processes are ceased. From the environmental aspect, there are several considerations of offshore jacket removal ideas, including conversion from an oil and gas rig into an artificial reef. The local law of California State now allows consideration of the RtR (Rig to Reef) scenario, conveying that RtR is one of the feasible methodologies to use the aged offshore platform. However, the RtR method will not be feasible if the local government law still insists that the jacket owner remove the platform [3].

The other options were being considered, including conversion from an oil and gas platform into an open ocean aquaculture platform. However, several liability issues still temporize the idea. Since the original jacket platform owner is never totally free of decommissioning obligations, owners may be unwilling to sell their facilities to aquaculture operators, hence deferring the economic benefit of aquaculture [4]. Due to the regulation, especially in Southeast Asia, decommissioning is an obligation to the operator. From the technical aspects, most of the study concluded that decommissioning the topside platform by complete removal to shore is the most worthy scenario, having fewer environmental effects than other removal scenarios, such as disposal onto the seabed. It also applied in jacket structure. Complete removal of the sore is the most reasonable scenario from an environmental point of view [5]. The complete removal of the topside and jacket is invariably done through the lifting process. Unlike the installation process, the decommissioning process reverts the installation process with lower acceptance criteria. However, safety consideration is still strictly applied. Even during the removal process, the "it is just a waste" mindset is strictly prohibited for the crew not to be less rigorous when handling the lifted jacket [6].

This paper investigates the barge motion's effect on the reversed process of the jacket lifting during

<sup>1</sup>Murdjito is with Departement of Ocean Engineering Institut Teknologi Sepuluh Nopember, Surabaya, 60111, Indonesia. E-mail: [murdjito@oe.its.ac.id](mailto:murdjito@oe.its.ac.id)

<sup>2</sup>Vebby A. Kurniawan is with Departement of Ocean Engineering Institut Teknologi Sepuluh Nopember, Surabaya, 60111, Indonesia. E-mail: [akbarvebby10@gmail.com](mailto:akbarvebby10@gmail.com)

<sup>3</sup>Raditya D. Riyanto is with Departement of Ocean Engineering Institut Teknologi Sepuluh Nopember, Surabaya, 60111, Indonesia. E-mail: [radityadanu@oe.its.ac.id](mailto:radityadanu@oe.its.ac.id)

<sup>4</sup>Rudi W. Prastianto is with Departement of Ocean Engineering Institut Teknologi Sepuluh Nopember, Surabaya, 60111, Indonesia. E-mail: [rudwp@oe.its.ac.id](mailto:rudwp@oe.its.ac.id)

decommissioning. The effect of the crane barge motion on the jacket lifting process is discussed.

## II. METHOD

### A. Fixed Offshore Facility Decommissioning

Several method options are available to be applied in the platform decommissioning. The selection process is mainly affected by HLV availability, environmental aspects, and, most importantly, the available budget. In some cases, one oil and gas company will wait for several platforms in an oilfield or gas field to be decommissioned to be economically feasible to operate. There are three main methods for performing platform decommissioning: Leave-in-place, Partial or complete removal, and Topple in-place [7]. The option to leave the non-operational platform and convert it into recreational or sporting facilities is the least costly option. However, the structural integrity of the platform should be examined thoroughly, including the risk of interfering the navigation. The potential hazard due to natural disaster and structural collapse shall also be considered. Partial or complete removal option is mainly affected by whether the structures will be reused or not. Complete removal option is selected if the case is to reuse the platform, especially the topside. This option involves a lot of heavy lifting operation, mainly related with moving the topside and jacket to the transportation barge. For topple in place method, structure's foundation or bottom part is made unstable so that the structure will subvert on its side and submerged. The toppled structure is mainly used as reef. Among the three options above, the most cost-consuming method is the option of complete removal. This study use the scenario of complete removal option.

The most cost-consuming part in platform decommissioning is lifting the structures and transferring them into a cargo barge, as shown in Table 1. Either be toppled in place or completely removed, the lifting operation is still to be performed. The cost is heavy on operation includes the daily lease rate for lifting vessel and cargo barge. Hence, the elaborative planning and engineering process of lifting operation is a mandatory. A perfectly engineered lifting plan can skimp the operation cost up to 30-70% [7].

Figure. 1 [8] shows the process of topside and jacket removal operation. Torches are generally used for cutting the weld connection between jacket and topside. The HLV lift the topside and transfer it into cargo barge. While the Before the jacket removal, the conductor and piles are severed using torches, mechanical cutting device or explosives to cut the connection with the jacket. Normally, it needs 5 meters under the seabed to cut the piles and conductors. After that, jacket is lifted into the barge or toppled in place. The decommissioning

process is divided into several operations [9]:

- 1) Pre-job activities. Before the execution of decommissioning, several pre-job activities are performed, including planning and engineering the decommissioning process. All information regarding platform historical data, including drawing, process flow diagrams and structural integrity documents, are gathered. Engineering is carried out to determine the exact procedures, vessels, equipment, and human resources that may be used during the decommissioning.
- 2) Well plugging and abandonment. The well that is no longer in production must be plugged to prevent the remaining oil and gas from leaking out the surface and contaminating the marine environment. The commonly used material in well plugging is cement, together with a bridge plug to completely shut-down the well production.
- 3) Pipeline decommissioning. Pipelines may be removed or abandoned in place with some requirements. Pipelines must be pigged and flushed with water. The site abandonment may be performed with strict regulation to be flushed, filled with seawater and the ends must be buried at least 1 m. The abandoned pipelines must not generate hazard to the environment, including navigation and other marine activities.
- 4) Platform decommissioning. The platform decommissioning operation covers the cleaning process, conductor removal, deck removal, and jacket removal. The platform must be cleaned from the remaining oil and gas substance, to prevent leakage during removal. The conductor, deck, and jacket are removed using Heavy Lift Vessel (HLV) to transportation barge and transported to the disposal site.
- 5) Disposal. The structural components of the jacket and topside are cut into small scrap pieces, while the equipment are reused whenever possible.
- 6) Site clearance and verification. Based on US Laws NTL No. 98-26 Minimum Interim Requirements for Site Clearance (and Verification) of Abandoned Oil and Gas Structures in the GOM, the site shall be cleared using trawlers that dragged across the seafloor and verified that there are no remaining debris. Other region, especially in Southeast Asia, may have different laws and obligation related to debris.
- 7) Post job activities. After the site is verified by the authorities, full report should be submitted to the government so that the platform owner is acknowledged to completely remove the

TABLE 1.  
 DECOMMISSIONING COST BREAKDOWN

No	Operation	Percentage to total cost
1	Lifting vessel and cargo barge	60%
2	Site clearance	18%
3	Decommissioning	11%
4	Mobilization and others	7%
5	Pipeline abandonment	4%



Figure 1. Topside Removal Using HLV and Jacket Removal Lifting Process

structures and the operating support system.

### B. Numerical Modelling

In this paper, a specific case is selected to demonstrate the planning and engineering process of lifting operation of jacket structure. L-Jacket, located in the Java Sea, is selected in this case study. L-Jacket is a four-legged jacket in 31.57m (103.57 ft) water-depth (Mean Sea Level). L Platform is one of 5 platforms operated in L Field, started in 1974. L Platform decommissioning plan is still under discussion, but the operation is preconcerted to execute in 2030 at most. The jacket elevation from the mudline is 38m, and at that height, the length at bay A-B is 11.73 m, whilst the length at bay 1-2 is 12.09 m. Figure. 2.(a) for details. Jacket length and width at elevation 38 m as depicted in Figure. 2.(b) is the measurement parameter to design the rigging arrangement. The structure includes only jacket

leg and bracing, with a total weight of 332.73 MT, and the Center of Gravity (CoG), measured from the bottom-center elevation of the jacket, is -0.22, 2, and 15.93 m respectively for X, Y, and Z-axis.

This study performs numerical modelling of HLV using hydrodynamics simulation software. Timas DLB 01 vessel is used for example to perform HLV modelling with properties as shown in Table 2 [10]. Timas DLB 01 is stern crane vessel with maximum boom height up to 84 m. Numerical validation of the HLV model is performed by comparing the displacement at the full draft from the vessel specification data and the linesplan model of the vessel. The vessel carried the jacket in her stern crane. The CoG is adjusted accordingly using HLV's ballast system. The numerical model is generated for hydrostatics and regular hydrodynamics analysis to perform RAO (Response Amplitude Operator) calculation. **Error! Reference source not found.** shows

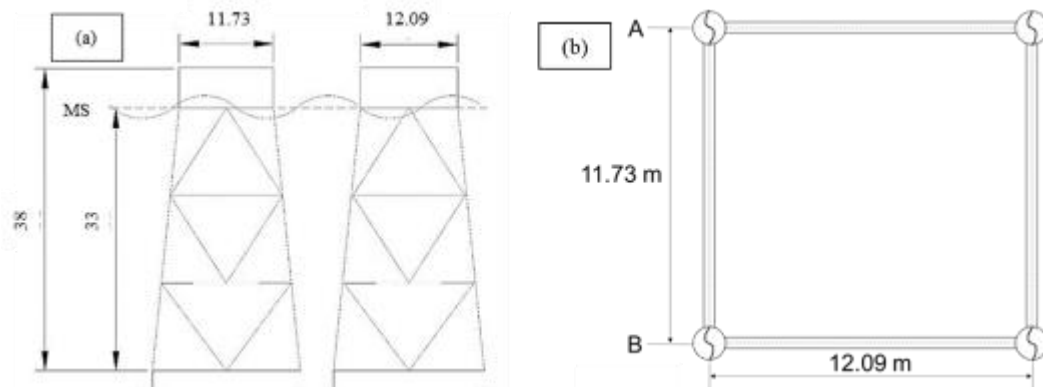


Figure 2. Jacket platform side view (a) and top view at elevation +38 m from mudline

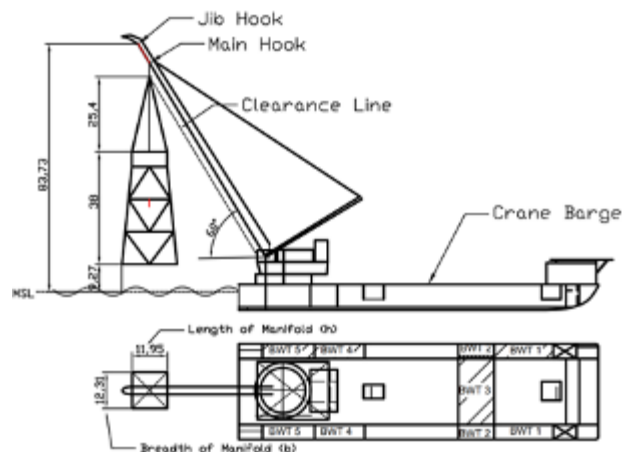


Figure 3. HLV and Jacket arrangement during decommissioning

TABLE 2.  
HLV PROPERTIES

Ship Particular	
LoA	121.9 m
Beam	32.3 m
Depth	8.7 m
Draft	4.3 m min / 5.5 m max
LWT+DWT	14,557 tonnes
Crane Specification	
Main Crane	American Model 509
Boom Length	84.0 m
Main Hook Capacity Fixed	816 MT
Main Hook Capacity Revolving	595 MT
Auxiliary Hook Capacity	272 MT
Whip Hook Capacity	136 MT / 47 MT

the final configuration for lifting arrangement of jacket and HLV in this case.

The lifted jacket motion is strictly related with the HLV motion, depicted by its RAO. The uni-fied motion of this two objects, namely jacket and HLV, when subjected to random wave load, will generate dynamic mo-tion response that can be expressed with Equation 1 [11].

$$[M]\{\ddot{X}\} + [C]\{\dot{X}\} + [K]\{X\} = \{F_w\} + \begin{matrix} R \\ (m, T, \delta_x, \delta_z, X_T, Y_T, Z_T) \end{matrix} \quad (1)$$

where [M], [C], [K], are the coefficient matrices of forces and moments for mass, damping and stiffness. {F<sub>w</sub>} is the exci-tation forces and moments generated by wave. R is the vector of reaction from lifted jacket which consists of jacket mass (m), sling tension (T), swing angles (δx and δz) and the displacement vector of crane boom tip which lifted the jacket (X<sub>T</sub>, Y<sub>T</sub>, Z<sub>T</sub>).

The displacement vector of crane boom tip is the interface point between the vessel and the jacket [12]. The jacket swing angles are in two direction (x and z) both for translation and rotation. This interface point is located at the boom tip and is expressed as below Equation 2[11]:

$$m \begin{pmatrix} \ddot{X}_L \\ \ddot{Y}_L \\ \ddot{Z}_L \end{pmatrix} = T \begin{pmatrix} -\sin\delta z & \cos\delta x \\ \sin\delta z & \sin\delta z \\ \cos\delta z & -\frac{mg}{T} \end{pmatrix} \quad (2)$$

In the initiation phase where the lifted jacket are assumed unified with the sheave and the acceleration of the vessel and jacket is considered equal, Equation 3 above can be re-expressed as below equation:

$$\begin{cases} \ddot{\delta x} \sin\delta z + 2\ddot{\delta x}\delta z - \frac{X_T}{l} \sin\delta x - \frac{Y_T}{l} \cos\delta x = 0 \\ \ddot{\delta z} - (\dot{\delta x})^2 \sin\delta z \cos\delta x + \frac{X_T}{l} \cos\delta z \cos\delta x \\ - \frac{Y_T}{l} \cos\delta z \sin\delta x + \frac{Z_T}{l} \sin\delta z + \frac{g}{l} \sin\delta z = 0 \end{cases} \quad (3)$$

Where l is the sling length and the tension occurred at the sling is mathematically expressed as Equation 4:

$$\frac{T}{m} = g \cos\delta z + l \{ (\dot{\delta z})^2 + (\dot{\delta x})^2 \sin(\delta z)^2 \} - \{ \ddot{X}_T \sin \delta z \cos\delta x - \ddot{Y}_T \sin \delta z \cos\delta x - \ddot{Z}_T \cos \delta z \} \quad (4)$$

### C. Environmental Modelling

Based on the referenced codes and rules [13] for short period marine operation in Java Seas, the environmental load follows the ‘benign all year’ criteria, as described a Table 3.

The wave spectra suitable for Indonesian waters is the JONSWAP wave spectra because of its archipelagic characteristics [14]. The JONSWAP spectra are based on experiments conducted in the North Sea. The JONSWAP spectrum equation can be written by modifying the Pierson-Moskowitz [15] spectrum equation namely shown in Equation 5.

$$S_j(\omega) = A_\gamma S_{pm}(\omega) \gamma^{\exp(-0.5(\frac{\omega-\omega_p}{\sigma\omega_p})^2)} \quad (5)$$

Where:

$S_j(\omega)$  : JONSWAP Spectra

$S_\zeta(\omega)$  : ISSC Spectra

$S_{pm}(\omega)$  : Pierson-Moskowitz spectra

$$\frac{5}{16} H_s^2 \omega_p^4 \omega^{-5} \exp(-\frac{5}{4}(\frac{\omega}{\omega_p})^{-4})$$

$\gamma$  : Peakness parameter

TABLE 3.  
ENVIRONMENTAL DATA

No.	Parameter	Data
1	Significant wave height (H <sub>s</sub> )	2.00 m
2	Current speed	0.50 m/s
3	Wind speed	15.00 m/s

- $\sigma$  : Shape parameter  
 $\omega \leq \omega_0 = 0.07$ ;  $\omega \geq \omega_0 = 0.09$
- $A_\gamma$  : normalizing factor =  $1 - 0.287 \ln(\gamma)$
- $\omega$  : wave frequency (rad/sec)
- $\omega_p$  : angular spectral peak frequency (rad/sec)
- $H_s$  : Significant wave height (m)
- $T_p$  : Peak-to-peak wave period (s)

- $LPT$  : Lifting point coordinate (m)
- $O$  : Center of Gravity (m)
- $\theta_i$  : Angle between hook point and lifted object plane (deg)
- $H_4$  : Distance between hook point and lifted object plane (m)
- $D_x$  : Distance between lift point in X direction (m)
- $D_y$  : Distance between lift point in Y direction (m)
- $W_m$  : Lifted structure width (m)
- $L_m$  : Lifted structure length (m)
- $\gamma$  : Tilting angle (deg)

**D. Rigging Arrangement Variation**

In this paper, several rigging arrangements for lifting operation are considered, in analyzing their sensitivity and obtain the best arrangement according to the applicable rules. Four lifting points are applied, with vertical lifting method selected for all variations. The sling length on all four lifting points are different. The variations and its respective theoretical formula [16] are described in following section.

Figure. 4(a) explains the general arrangement of single hook rigging without spreader bar (Rigging#1). The lifting calculation is described at Equation 6-9.

$$L_i = \sqrt{H^2 + (LPT - O)^2} \quad (6)$$

$$\theta_i = \cos^{-1} \left( \frac{\sqrt{\left(\frac{D_x}{2} - \frac{W_h}{2}\right)^2 + \left(\frac{D_y}{2} - \frac{L_h}{2}\right)^2}}{L_i} \right) \quad (7)$$

$$H_4 = \left( \sqrt{(L_1)^2 - \left(\frac{D_x}{2} - \frac{W_h}{2}\right)^2 + \left(\frac{D_y}{2} - \frac{L_h}{2}\right)^2} \right) \quad (8)$$

$$\gamma \approx 0 \quad (9)$$

where:

- $L_i$  : Sling length at  $i$  point (m)

Figure. 4 (b) shows the general arrangement of single hook rigging with single spreader bar (Rigging#2). The lifting parameter is calculated based on Equation 10-13.

$$\theta = \cos^{-1} \left( \frac{\sqrt{\left(\frac{D_x}{2}\right)^2 + \left(\frac{D_y}{2} - \frac{L_{SP}}{2}\right)^2}}{L'} \right) \quad (10)$$

$$\gamma = \cos^{-1} \left( \frac{\sqrt{\left(\frac{L_{SP}}{2} - \frac{L_h}{2}\right)^2}}{L'} \right) \quad (11)$$

$$H_4 = \left( \sqrt{(L')^2 - \left(\frac{D_x}{2}\right)^2 - \left(\frac{D_y}{2} - \frac{L_{SP}}{2}\right)^2} \right) \quad (12)$$

$$H_5 = \left( \sqrt{(L'')^2 - \left(\frac{L_{SP}}{2} - \frac{L_h}{2}\right)^2} \right) \quad (13)$$

where:

- $L''$  : Sling length above spreader bar (m)
- $L'$  : Sling length below spreader bar (m)
- $L_h$  : Length of hook block (m)

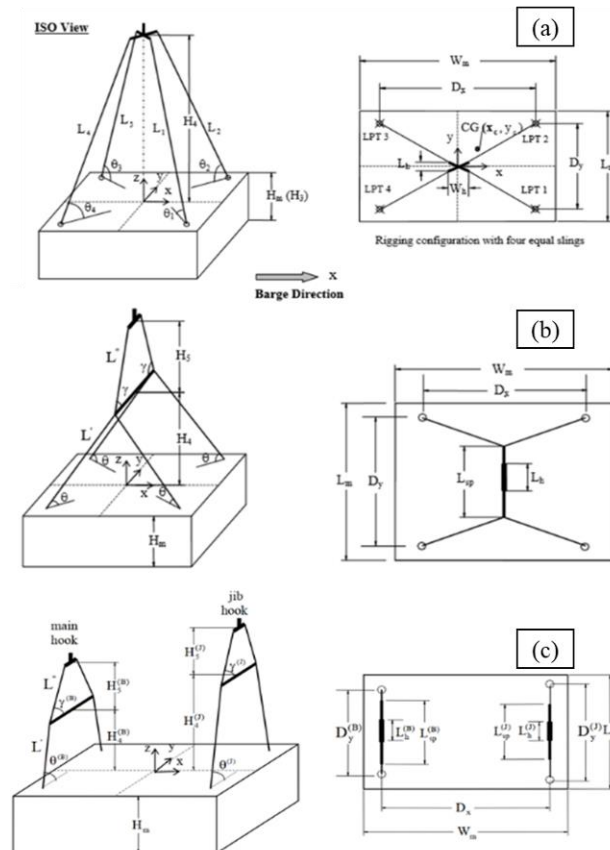


Figure. 4. Rigging arrangements

- $L_{SP}$  : Length of spreader bar (m)
- $\theta$  : Angle between sling and lifted object plane (deg)
- $\gamma$  : Tilting angle (deg)
- $H_4$  : Vertical distance between hook point and spreader bar (m)
- $H_5$  : Vertical distance between spreader bar and lifted object plane (m)

The third arrangement consists of four lifting point with double hook (Rigging#2), one acts as main hook and second acts as jib hook as shown on Figure. 4(c). The lifting calculation is shown in Equation 14-17.

$$\theta^B = \cos^{-1} \left( \frac{D_y^{(B)} - L_{sp}^{(B)}}{2L'} \right) \quad (14)$$

$$\gamma^B = \cos^{-1} \left( \frac{L_{sp}^{(B)} - L_h^{(B)}}{2L''} \right) \quad (15)$$

$$H_4^{(B)} = \sqrt{(L')^2 - \left( \frac{D_y^{(B)}}{2} - \frac{L_{sp}^{(B)}}{2} \right)^2} \quad (16)$$

$$H_5^{(B)} = \sqrt{(L'')^2 - \left( \frac{L_{sp}^{(B)}}{2} - \frac{L_h^{(B)}}{2} \right)^2} \quad (17)$$

### III. RESULTS AND DISCUSSION

#### A. HLV Response Amplitude Operator

When a vessel is subjected to waves from specific attack angle, the vessel will respond in form of motion. Each vessel generates unique response even when subjected to the same waves. The set of responses in six degree of freedom (Surge, Sway, Heave, Roll, Pitch, and Yaw) are referred as Response Amplitude Operator (RAO) [17].

From Figure. 5, the beam seas waves (90-degree wave attack angle) produce the most significant motion in sway, roll, and yaw RAO. In swaying motion, a 1 m wave at an angular frequency of 0.5 rad/s creates a 1.8 m HLV response. In rolling motion, a 1 m wave at angular frequency 0.55 rad/s creates 3.5 degrees HLV response. In yawing motion, a 1 m wave at an angular frequency of 0.6 rad/s creates 1.9 degrees of response.

While for following and head seas waves (180 and 0 degrees wave attack angle, respectively) produce the most significant motion in the surge, heave and pitch RAO as shown in Figure. 5. In surging motion, a 1 m wave at an angular frequency of 0.3 rad/s also creates a 1 m HLV response. In heaving motion, a 1 m wave at an

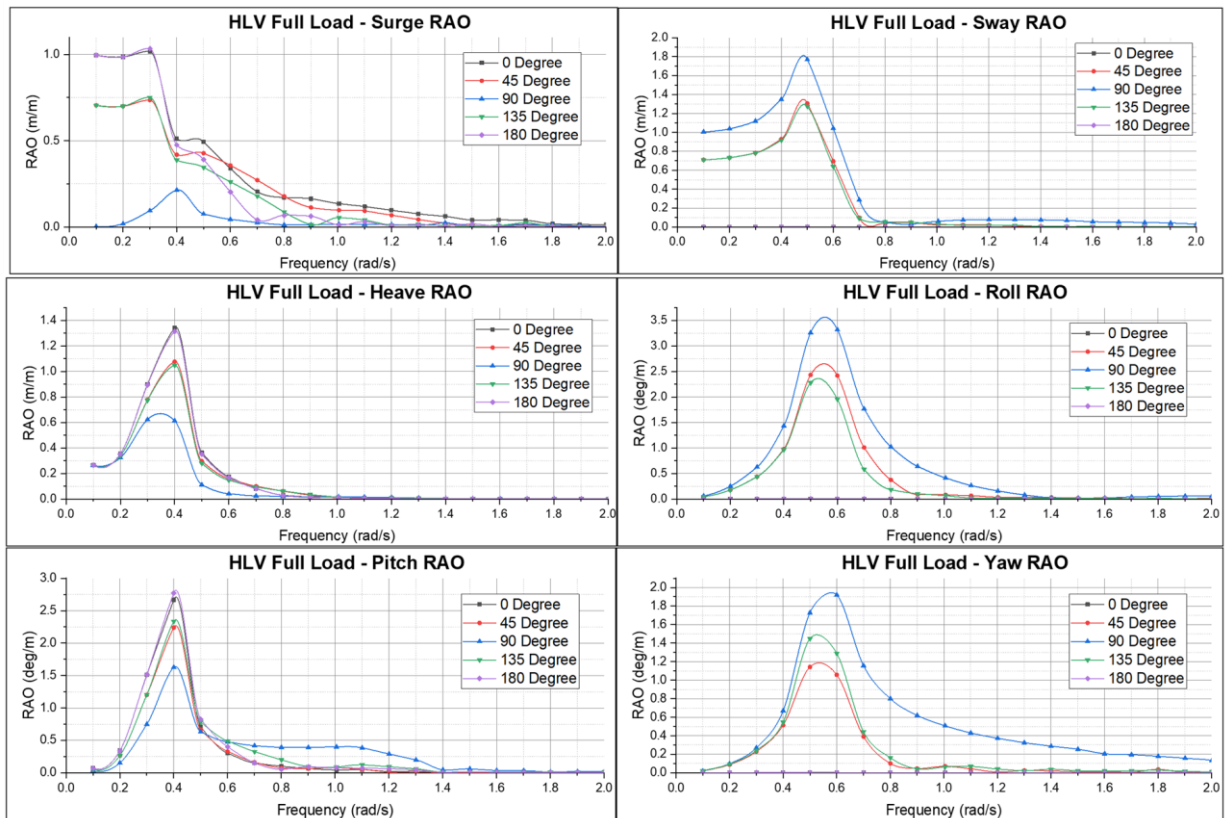


Figure. 5. Full Load RAO of HLV in surge, sway, heave, roll, pitch, yaw

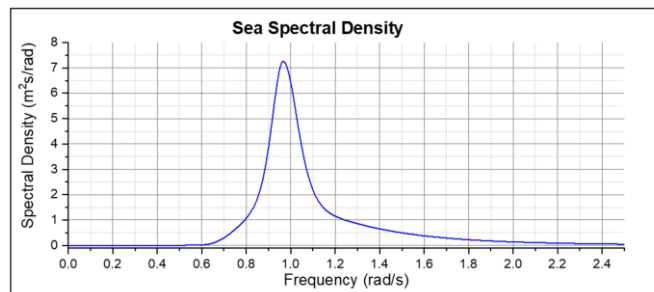


Figure. 6. Sea spectral density

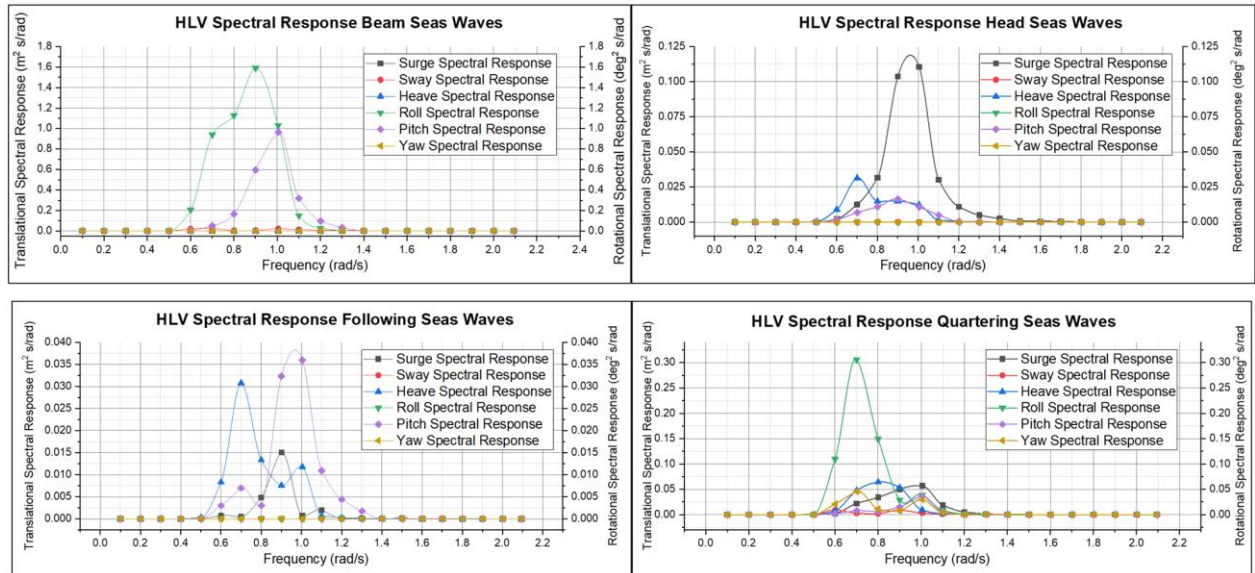


Figure 7. HLV Spectral Response for Beam, Head, Following, and Quartering Seas Waves

angular frequency of 0.4 rad/s creates a 1.3 m HLV response. In pitching motion, a 1 m wave at an angular frequency of 0.4 creates a 2.75-degree response.

The maximum values of these responses occur at low-frequency waves, i.e., 0.3 to 0.5 rad/s. Indonesian seas are generally closed seas with medium to high frequency, the random seas using JONSWAP spectra, and the spectral density result is described in Figure. 6. It can be seen that the densest wave occurred at an angular frequency of 0.8 to 1.2 rad/s; hence the amplitude magnification of the HLV motion does not likely occur due to the different wave frequency region.

### B. HLV Spectral Response

3 hours of simulation (10,800 seconds) is performed to analyze the dynamic behavior of the HLV and the lifted jacket during decommissioning. This section explains the HLV spectral response for all rigging variations for beam seas, head seas, following seas and quartering seas.

Fig. 13 below depicts the HLV response when subjected to beam seas waves. It can be seen that the most dominant motion for beam seas waves is roll and the second most dominant is pitch. HLV responses the beam seas with rolling motion both in the region of its natural frequency, namely 0.4 to 0.5 rad/s and the wave spectra densest region, namely in 0.8 to 1.2 rad/s. However, waves apparently play more dominant role in spectral response, it can be seen from the graph that the peak of the spectral response is in 0.9 rad/s. Fig. 14 below explains the HLV spectral response when encountered to head seas waves, with the most dominant motion in surge response. The peak of the response is in the region of sea spectral density namely at 0.8 to 1.0 rad/s.

Fig. 15 below explains the HLV spectral response when exposed to following seas waves. It shows two

dominant responses in different wave frequency region. Heave response is second most dominant with spike of the response is in the region of the HLV natural frequency. Pitch response is the most dominant HLV response in the region of densest wave energy in 0.8 to 1.2 rad/s frequency. Again, wave apparently plays more dominant role in following seas spectral response, looking at the highest spike is at 0.9 to 1.0 rad/s frequency. HLV spectral response in quartering seas are dominated by the roll motion at its natural frequency region, as shown in Fig. 16. There is little influence in sea energy, looking at the figure that shows no spike in the region of wave densest energy, in 0.8 to 1.2 rad/s. The peak of the roll spectral response is in 0.7 rad/s.

Table 4 shows the summary of the HLV spectral response. It can be inferred that the sea energy density plays a significant role in determining HLV spectral response. This tendency is shown by how the HLV responded while encountered by beam seas, head seas, and following seas waves. An exception occurs on HLV spectral response to quartering seas waves. The response is dominated by the roll motion on the region of her natural frequency.

### C. Jacket Relative Motion

The jacket relative motion is the measurement of the jacket's center of gravity motion relative to its initial position. The response spectra for dominant motions are reported and briefly discussed in this section. The response that has a higher graph is interpreted as having a greater response, so it is assumed that it is more unsuitable for application in the field.

For beam seas waves, the dominant jacket motion is in Z-translation and X-rotation. The jacket motion is highly related to the HLV motion, as it can be observed from Figure. 7 that the most dominant HLV response is in roll (X-rotation) and pitch (Y-rotation) motion. Figure.

TABLE 4.

SPECTRAL RESPONSE SUMMARY

Wave direction	Dominant response	Frequency region
Beam seas	Roll (X-rotation)	Wave dominant
Head seas	Surge (X-translation)	Wave dominant
Following seas	Pitch (Y-rotation)	Wave dominant
Quartering seas	Roll (X-rotation)	HLV natural freq.

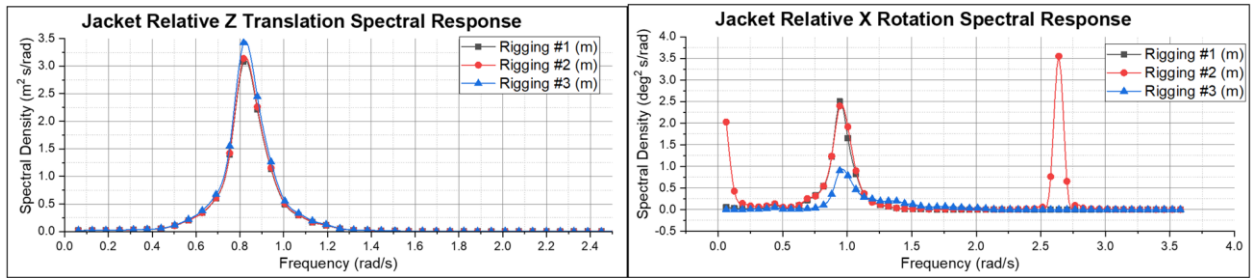


Figure 8. Jacket relative z-translation and x-rotation spectral response beam seas waves

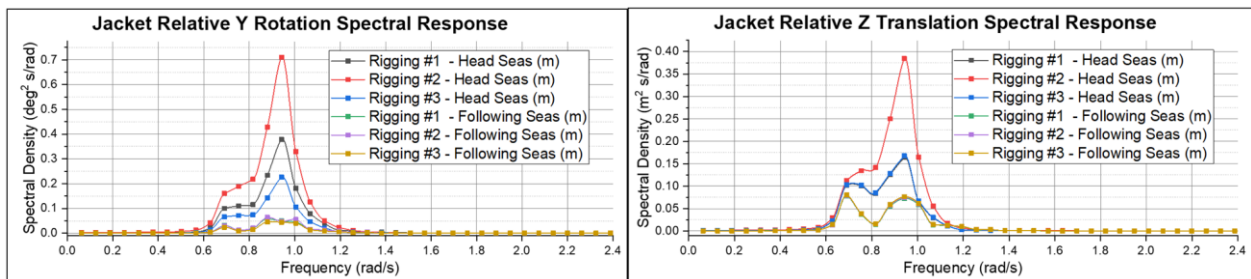


Figure 9. Jacket relative y-rotation and z-translation spectral response head seas and following seas waves

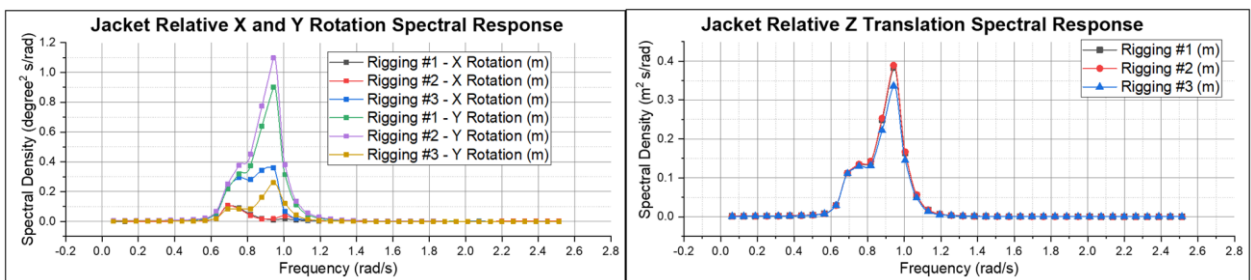


Figure 10. Jacket relative x-y-rotation and z-translation spectral response quartering seas waves

8 explains the spectral response of the jacket relative to Z-translation and X-rotation. While the largest response is generated by Rigging #3, the other arrangement variations show a relatively similar result. The maximum value of the response is averagely 1.55 m for these three variations, whereas the most probable value of Z translation is averagely 1.22 m. For X-rotation, all rigging variations, the first spike in response occurs in the wave densest region, namely at 0.9 to 1.1 rad/s. From the figure, we can also examine that Rigging #2 has the largest response, which has three total spikes. The first spike is at the low-frequency region, the second is at the wave energy region, and the third spike is at the high-frequency wave. In fact, the third spike is the highest response.

This phenomenon shows that the spreader bar arrangement is not a good option when encountered by the high-frequency waves from beam seas, especially in X-rotation. For Rigging #2, the maximum value of the response is 3.06 degrees, whilst the most probable response is 2.52 degrees.

For head seas following seas waves, the responses are significantly lower and do not closely relate with the vessel motion. Head seas and following seas waves generate dominant surge (X-translation) and pitch (Y-rotation) HLV response, respectively. However, the dominant jacket motion is in Y-rotation motion and Z-translation. Even though it is significantly lower, the response from these two types of encountering direction

is important to be investigated, as the crane of HLV used in this study is in her stern, a wave coming from the head and following seas is very important to consider.

Figure 9 portrays the jacket relative Y-rotation and Z-translation when the HLV is attacked by head seas and following seas waves. The response spiked at the frequency of the wave and vessel. The maximum statistical value of Rigging #2 for its Z-translation is 0.41 m, while its most probable value is 0.32 m. The Y-rotation statistical maximum value is 0.62 degree, and the most probable value is 0.49 degree. The response spiked at both HLV and wave frequency, namely 0.6 to 1.2 rad/s, with the peak is at 0.9 rad/s, similar to the peak frequency of the wave spectra. It can be concluded that Rigging #2 has the largest response spectra, while Rigging #3 has a predominantly lower response both from head seas and following seas waves. Similar to previous waves encountering direction, in this paper, the spreader bar again showed a generally worst response among the variations simulated.

For quartering seas waves, where the waves attack the vessel from 45 degrees from forward, the HLV generates X-rotation dominant response in her natural frequency region. However, it turns out that the jacket does not respond in the same motion and frequency as the HLV. The dominant jacket response is in Y-rotation and Z-translation.

The quartering sea responses are more influenced by the resultant of the jacket response in beam seas and

Table 5.  
JACKET RELATIVE MOTION RESPONSE SUMMARY

Wave direction	Jacket response	Predominantly influenced by	Frequency Region
Beam seas	dZ and rX	HLV motion	Wave dominant
Head & following seas	dX and rY	Wave encountering energy	Wave dominant
Quartering seas	dZ and rY	Wave encountering energy	Wave dominant

head seas other than the HLV motion. It can be observed in Figure. 10, the jacket generates responses in the wave densest energy region, namely from 0.8 to 1.2 rad/s, and the X-rotation response is significantly smaller than its Y-rotation. The maximum statistical value of Y-rotation is 1.49 degrees, while its most probable value is 1.33 degrees. For Z-translation, the maximum statistical value is 0.53 m, and the most probable value is 0.44 m.

The summary of the jacket relative motion response is described in Table 5. The result indicates that the motion of the lifted jacket during decommissioning when encountered by beam seas waves is influenced by the HLV motion. While the jacket motion when the HLV exposed to head seas, following seas and quartering seas waves are mostly affected by wave encountering energy rather than HLV motion.

#### IV. CONCLUSION

In this paper, we investigate the effect of barge motion on a decommissioned jacket during the lifting phase. The regular wave response of the HLV (Heavy Lift Vessel) was calculated using numerical software. While the random wave response for three rigging arrangements and four-wave encountering angles were performed. A coupled analysis between wave energy, HLV response spectra, and jacket motion spectra has been presented in this paper. JONSWAP spectrum for closed seas was used in this paper with high frequency and low wave characteristics, similar to Indonesian waters.

From the analysis performed, it is found that the vessel has a more sensitive response in wave energy frequency rather than in its natural frequency, although the wave energy is relatively small. The same motion result happened for jacket relative motion response, where for the head, following, and quartering seas, jacket motions are predominantly influenced by wave energy rather than HLV motion. An exception occurred for beam seas waves where the jacket responded more from the HLV motion. All of these motions occur at the frequency where the wave densest energy region takes place.

#### ACKNOWLEDGEMENTS

Authors would like to express their sincere gratitude Directorate of Research and Community Service of Institut Teknologi Sepuluh Nopember (ITS) Surabaya to support the funding of this research. Authors also would like to express their gratitude to ZEE Engineering for providing the simulation workspace and guidance during the research.

#### REFERENCES

[1] International Energy Agency, "Southeast Asia Energy Outlook 2019," Paris, 2019.

[2] M. J. Kaiser and M. Liu, "Decommissioning cost estimation in the deepwater U.S. Gulf of Mexico - Fixed platforms and compliant towers," *Mar. Struct.*, vol. 37, pp. 1–32, 2014, doi: 10.1016/j.marstruc.2014.02.004.

[3] A. S. Bull and M. S. Love, "Worldwide oil and gas platform decommissioning: A review of practices and reefing options," *Ocean and Coastal Management*, vol. 168, pp. 274–306, 2019, doi: 10.1016/j.ocecoaman.2018.10.024.

[4] M. J. Kaiser, B. Snyder, and Y. Yu, "A review of the feasibility, costs, and benefits of platform-based open ocean aquaculture in the Gulf of Mexico," *Ocean and Coastal Management*, vol. 54, no. 10, Elsevier Ltd, pp. 721–730, 2011, doi: 10.1016/j.ocecoaman.2011.07.005.

[5] P. Ekins, R. Vanner, and J. Firebrace, "Decommissioning of offshore oil and gas facilities: A comparative assessment of different scenarios," *J. Environ. Manage.*, vol. 79, no. 4, pp. 420–438, 2006, doi: 10.1016/j.jenvman.2005.08.023.

[6] C. White and G. Adams, "North West Hutton decommissioning - A major challenge...a major success," in *Society of Petroleum Engineers - SPE/APPEA Int. Conference on Health, Safety and Environment in Oil and Gas Exploration and Production 2012: Protecting People and the Environment - Evolving Challenges*, 2012, vol. 2, pp. 1212–1229.

[7] A. Ali and A. Alghamdi, "Decommissioning Of Offshore Structures: Challenges And Decommissioning of Offshore Structures: Challenges," in *International Conference on Computational Methods in Marine Engineering*, 2005, no. June 2005.

[8] M. J. Kaiser, B. Snyder, and A. G. Pulsipher, *Assessment of opportunities for alternative uses of hydrocarbon infrastructure in the Gulf of Mexico*. Louisiana: U.S. Dept. of the Interior, Bureau of Ocean Energy Management, Regulation and Enforcement, Gulf of Mexico OCS Region, New Orleans, LA. OCS Study BOEMRE 2011-028. 278 pp, 2011.

[9] R. Grismala, "Decommissioning Methodology and Cost Evaluation," Fairvax, VA, 2015.

[10] Timas Suplindo, "DLB-01 Specification," *DLB-01 Specification*, 2020.

[11] K. Sekita, H. Kimura, and M. Tatsuta, "Dynamic lifting analysis of offshore structures," *Otc'86 Proc., Eighteenth Annu. Offshore Technol. Conf., (Houston, U.S.a. May 5-8, 1986)*, vol. 3, Richar, pp. 547–554, 1986.

[12] J. H. Cha, M. Il Roh, and K. Y. Lee, "Dynamic response simulation of a heavy cargo suspended by a floating crane based on multibody system dynamics," *Ocean Eng.*, vol. 37, no. 14–15, pp. 1273–1291, 2010, doi: 10.1016/j.oceaneng.2010.06.008.

[13] Det Norske Veritas, *Environmental conditions and environmental testing*, vol. 2, no. October. Høvik, Norway, 2010, doi: 10.1109/INTLEC.1993.388591.

[14] D. Adrianto, E. B. Djatmiko, and Suntoyo, "The improvement of ultrasonic sensor-based device for direct ocean wave measurement program at Western Java Sea-Indonesia," *IOP Conf. Ser. Earth Environ. Sci.*, vol. 389, no. 1, 2019, doi: 10.1088/1755-1315/389/1/012022.

[15] DNVGLND, *DNVGL-ST-N001-Marine-Operations - Det Norske Veritas*. 2016.

[16] L. Liang, *Heavy Lift Installation Study of Offshore Structures (Master Thesis)*. Singapore: Department of Civil Engineering, National University Singapore, 2004.

[17] P. Aird, "Chapter 4 - Deepwater Metocean Environments," in *Deepwater Drilling*, P. Aird, Ed. Gulf Professional Publishing, 2019, pp. 111–164, doi: https://doi.org/10.1016/B978-0-08-102282-5.00004-1.